

# B<sub>4</sub>C–CrB<sub>2</sub> composites with improved mechanical properties

Suzuya Yamada<sup>a,\*</sup>, Kiyoshi Hirao<sup>b</sup>, Yukihiro Yamauchi<sup>b</sup>, Shuzo Kanzaki<sup>b</sup>

<sup>a</sup>Synergy Ceramics Laboratory, Fine Ceramics Research Association, 2268-1, Shimo-Shidani, Moryama-Ru, Nagoya, Aichi, 463-8687 Japan

<sup>b</sup>Synergy Materials Research Center, National Institute of Advanced Industrial Science and Technology Nagoya, Aichi, 463-8687 Japan<sup>1</sup>

Received 28 December 2001; received in revised form 3 April 2002; accepted 11 April 2002

## Abstract

B<sub>4</sub>C based ceramic composites with 0–25 mol% CrB<sub>2</sub> were fabricated by hot-pressing at 1900 °C, and their mechanical properties were examined. The B<sub>4</sub>C–CrB<sub>2</sub> composites with both high strength of 630 MPa and modest fracture toughness of 3.5 MPa m<sup>1/2</sup> could be obtained by the addition of 20 mol% CrB<sub>2</sub>. It seems that improvement in fracture toughness is due to the formation of microcracks and deflection of propagating cracks caused by the thermal expansion mismatch between CrB<sub>2</sub> and B<sub>4</sub>C. © 2002 Elsevier Science Ltd. All rights reserved.

**Keywords:** B<sub>4</sub>C; Composites; Strength; Toughness and toughening; CrB<sub>2</sub>

## 1. Introduction

Due to their excellent properties such as high hardness, high elastic modulus, wear resistance, high melting point, low density and good chemical stability, boron carbide (B<sub>4</sub>C) based ceramics have good potential for various industrial fields.<sup>1–4</sup> However, the major problems with B<sub>4</sub>C based ceramics are their relatively low strength and fracture toughness as well as poor sinterability, caused by the low self-diffusion coefficient. Several additives have been examined to promote the densification of B<sub>4</sub>C. The effect of carbon addition on the densification of B<sub>4</sub>C has been reported.<sup>5–9</sup> A relative density of 96.4% was obtained by pressureless sintering of B<sub>4</sub>C doped with carbon at 2150 °C. Full densification was achieved by means of post-HIP treatment of the specimens. The flexural strength and the fracture toughness of the post-HIP specimen were 579 MPa and 2.4 MPa m<sup>1/2</sup>, respectively.<sup>9</sup> It was reported that Al and Al containing compounds such as AlF<sub>3</sub> are also effective additives for densification of B<sub>4</sub>C. For example, high relative density of 95% was achieved for B<sub>4</sub>C with the addition of 1 mass% Al by pressureless sintering at 2200 °C.<sup>10</sup> Kim et al. stated that the addition of a small amount of Al<sub>2</sub>O<sub>3</sub> greatly improved the sinterability of

B<sub>4</sub>C, and that a flexural strength of 550 MPa was obtained for a B<sub>4</sub>C based ceramic hot-pressed at 2000 °C with the addition of 2.5 vol.% Al<sub>2</sub>O<sub>3</sub>.<sup>12</sup> The effect of other additives such as SiC, TiC, WC and BN have also been investigated, with limited success.<sup>11,13–15</sup>

The purpose of these investigations was mainly to enhance the densification and, thereby, to increase the strength of B<sub>4</sub>C ceramics. B<sub>4</sub>C ceramics with dispersed TiB<sub>2</sub> particles have been investigated in order to increase both strength and toughness.<sup>16–20</sup> The improvement of fracture toughness was accomplished in terms of microcracking formation caused by the thermal expansion mismatch between dispersed particles and the matrix. Skorokhod and Krstic reported that a flexural strength of 621 MPa and a fracture toughness of 6.1 MPa m<sup>1/2</sup> were obtained for a B<sub>4</sub>C–15 vol.% TiB<sub>2</sub> composite produced by reaction hot-pressing of B<sub>4</sub>C with the addition of TiO<sub>2</sub> and C at 2000 °C.<sup>20</sup> The high strength of this material was attributed to the combination of high fracture toughness and fine microstructure.

The addition of CrB<sub>2</sub> is expected to be more effective for increasing the fracture toughness of B<sub>4</sub>C ceramics because of the larger difference in thermal expansion between B<sub>4</sub>C and CrB<sub>2</sub> than B<sub>4</sub>C and TiB<sub>2</sub>.<sup>1</sup> In addition, CrB<sub>2</sub> exhibits high hardness, high melting point and chemical stability.<sup>21–22</sup> B<sub>4</sub>C and CrB<sub>2</sub> phases can coexist according to the phase diagram of the B<sub>4</sub>C–CrB<sub>2</sub> system.<sup>23</sup> However, mechanical properties of B<sub>4</sub>C–CrB<sub>2</sub> ceramics have not been investigated. In the present

\* Corresponding author. Tel.: +81-52-739-0152; fax: +81-52-739-0051.

E-mail address: su-yamada@aist.go.jp (S. Yamada).

<sup>1</sup> Formerly, National Industrial Research Institute of Nagoya

study,  $B_4C$  ceramics with dispersed  $CrB_2$  particles were fabricated by hot-pressing a powder mixture of fine  $B_4C$  powder and  $CrB_2$ , and the microstructure and mechanical properties of the specimens were examined and compared with monolithic  $B_4C$ .

## 2. Experimental procedure

The  $B_4C$  starting powder (Grade No. 1500, Denki Kagaku Kogyo Co., Tokyo, Japan) has an average particle size of 0.40  $\mu m$  and a specific surface area of 22.4  $m^2/g$ . The powder contains oxygen (3.6 mass%), Fe (4000 ppm), and Al (1100 ppm) as impurities. The  $B_4C$  powder was mixed with  $CrB_2$  powder with an average particle size of 3.5  $\mu m$  (Japan New Metals Co., Osaka, Japan) using a planetary ball mill with a SiC pot and SiC balls in methanol for 30 min. The chromium diboride content was varied from 5 to 25 mol%. The slurry was dried in a rotary vacuum evaporator for 1 h, followed by oven drying at 115  $^{\circ}C$  for 24 h. The powder mixture was passed through a 60 mesh sieve. Hot-pressing was performed using a carbon resistance furnace in a rectangular graphite die (47 $\times$ 42 mm) at 1900  $^{\circ}C$  for 1 h with an applied load of 50 MPa under 0.1 MPa argon pressure. The temperature was monitored by an optical pyrometer which was calibrated in advance using a thermocouple. The heating rates were 40  $^{\circ}C/min$  from room temperature to 1200  $^{\circ}C$ , 20  $^{\circ}C/min$  to 1500  $^{\circ}C$  and 10  $^{\circ}C/min$  to 1900  $^{\circ}C$ . For the sake of comparison,  $B_4C$  specimen without  $CrB_2$  was also fabricated by the same procedure.

For measuring mechanical properties, test pieces were cut from the hot-pressed specimens and ground with a 400-grit diamond wheel to dimensions of 42 $\times$ 4 $\times$ 3 mm. The flexural strength was measured by a four-point bending test with inner and outer spans of 10 and 30 mm, respectively. The fracture toughness,  $K_{IC}$ , was measured by the SEPB method.<sup>24</sup> The densities of test pieces were determined by the Archimedes' method. Phase identification was performed by X-ray diffractometry (XRD: RINT 2500, Rigaku Co, Tokyo,

Japan) with  $CuK_{\alpha}$  radiation. In order to observe the microstructure, specimens were polished with 1  $\mu m$  diamond slurry. Some specimens were etched with Murakami's reagent (10 g of NaOH and 10 g of  $K_3Fe(CN)_6$  in 100 mL  $H_2O$  at 110  $^{\circ}C$ ). Microstructural analysis was carried out using scanning electron microscopy (SEM: JSM5600, Jeol Ltd., Tokyo, Japan). The mean grain size of  $B_4C$  was measured using image analysis (Scion Image, Scion Co., Maryland, USA).

## 3. Results and discussion

Table 1 shows the starting compositions and densities of the hot-pressed specimens. High relative density of 99.0% was achieved even in the specimen without  $CrB_2$ . Although relative densities of the specimens with up to 20 mol% the addition of  $CrB_2$  were higher than 99% of theoretical densities,  $B_4C$  with 25 mol%  $CrB_2$  was slightly lower than 99%.

The specimen without  $CrB_2$  was composed of fine equiaxed grains as shown in the etched surface of the specimen (Fig. 1). The grain size of  $B_4C$  is 0.93  $\mu m$  ( $\sigma$ : 0.28) in diameter. The development of such a fine microstructure is ascribed to the use of fine  $B_4C$  powder with an average particle size of 0.40  $\mu m$  and the relatively low sintering temperature of 1900  $^{\circ}C$  preventing substantial grain growth. Fig. 2 shows microstructures of  $B_4C$ –5 mol%  $CrB_2$ ,  $B_4C$ –20 mol%  $CrB_2$ , and  $B_4C$ –25 mol%  $CrB_2$  specimens observed in the polished surfaces of the specimens. The  $CrB_2$  particles appear as areas of high contrast in the darker  $B_4C$  matrix. It can be seen that  $CrB_2$  particles of a few micron size are dispersed in the  $B_4C$  matrix. It is apparent that the average interparticle spacing between  $CrB_2$  particles decreases as the  $CrB_2$  volume fraction increases as shown in Fig. 2. In order to clarify the grain morphology of the  $B_4C$  matrix in the composites, chemical etching was conducted. Fig. 3 shows a polished and chemically etched

Table 1  
Starting compositions and densities of  $B_4C$  based specimens

	$CrB_2$ content		Theoretical density (g/cm <sup>3</sup> )	Measured density (g/cm <sup>3</sup> )	Relative density (%)
	(mol%)	(vol.%)			
(1)	0	0	2.52	2.50	99.0
(2)	5	3.1	2.61	2.60	99.6
(3)	10	6.2	2.71	2.70	99.7
(4)	15	9.6	2.82	2.79	99.0
(5)	20	13.0	2.92	2.89	99.0
(6)	25	16.7	3.03	2.99	98.6

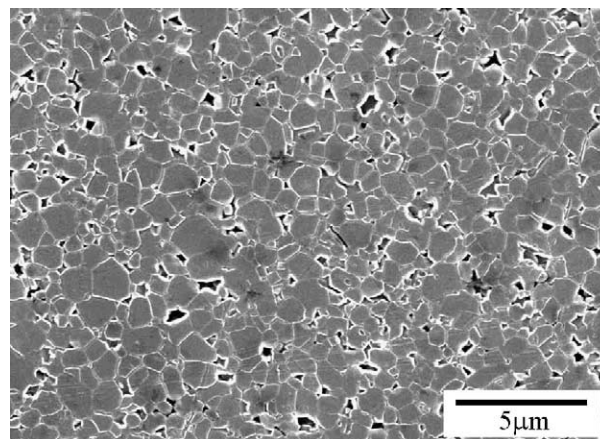


Fig. 1. Microstructure of specimen without  $CrB_2$ .

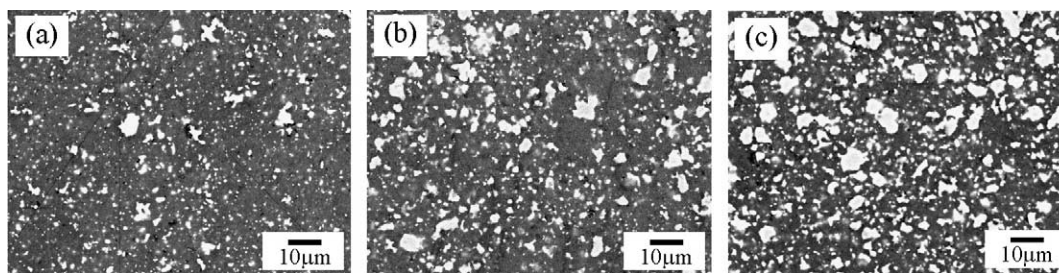


Fig. 2. Microstructures of  $B_4C$ - $CrB_2$  specimens: (a)  $B_4C$ -5 mol%  $CrB_2$ , (b)  $B_4C$ -20 mol%  $CrB_2$  and (c)  $B_4C$ -25 mol%  $CrB_2$ .

surface of the  $B_4C$ -20 mol%  $CrB_2$  specimen. Large pores were formed by dissolution of  $CrB_2$  during etching. The grain size of the  $B_4C$  matrix is  $1.0 \mu m$  ( $\sigma$ : 0.32) in diameter which is similar to that of the specimen without  $CrB_2$ .

Fig. 4 shows X-ray diffraction spectra of the specimens. For the specimen without  $CrB_2$ , only the  $B_4C$  phase was identified except for a small peak at  $35.7^\circ$  which corresponds to diffraction from 6H-SiC (102). This SiC contamination is thought to originate from the SiC pot and balls during mixing. XRD analysis of the  $B_4C$ -5 mol%  $CrB_2$  and  $B_4C$ -20 mol%  $CrB_2$  specimens

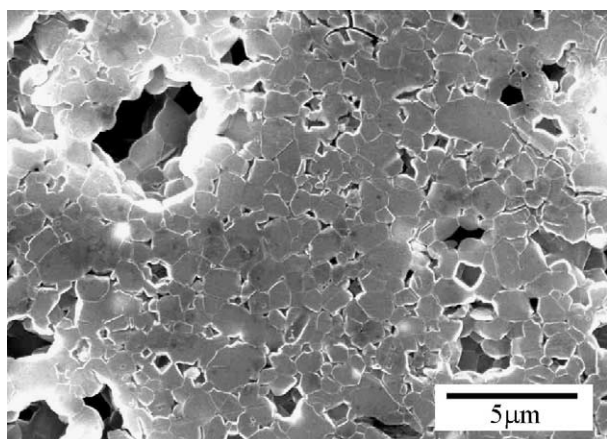


Fig. 3. Microstructure of  $B_4C$ -20 mol%  $CrB_2$  specimen.

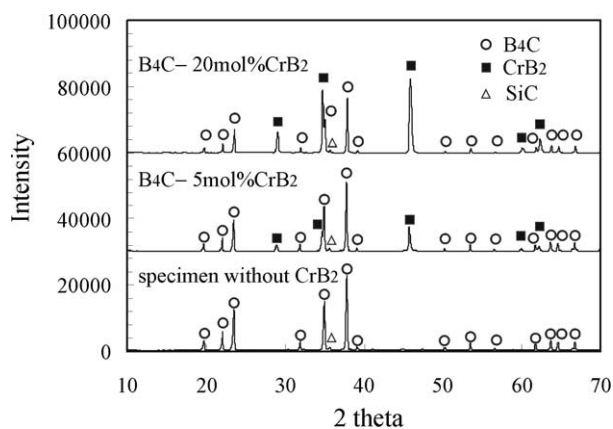


Fig. 4. X-ray diffraction spectra of specimen without  $CrB_2$  and  $B_4C$ - $CrB_2$  specimens.

revealed that they were composed of  $B_4C$  and  $CrB_2$  phase with trace of SiC. No other phase was identified.

The flexural strength and fracture toughness of the specimens as a function of  $CrB_2$  content are shown in Fig. 5. The fracture toughness of the specimen without  $CrB_2$  was as low as  $2.5 \text{ MPa m}^{1/2}$ . The fracture toughness increased to  $3.5 \text{ MPa m}^{1/2}$  with increasing the  $CrB_2$  content up to 20 mol% (13 vol.%), and thereafter decreased slightly (Fig. 5b). Fig. 6 shows fractured surfaces of the specimen without  $CrB_2$  and the  $B_4C$ -20 mol%  $CrB_2$  specimen. The fracture surface of the specimen without  $CrB_2$  was quite smooth owing to the transgranular mode of fracture. It is considered that the transgranular mode of fracture resulted in the low fracture toughness of the specimen. On the contrary, the fracture surface of the  $B_4C$ -20 mol%  $CrB_2$  specimen was relatively rough. It is clearly seen that  $CrB_2$  particles are dispersed in the fine grained  $B_4C$  matrix. The  $B_4C$  matrix fractured transgranularly, whereas intergranular fracture occurred partially at the interfaces between the  $CrB_2$  particles and the  $B_4C$  matrix. It appears that this change of fracture mode by the addition of  $CrB_2$  gives rise to the improvement of the fracture toughness.

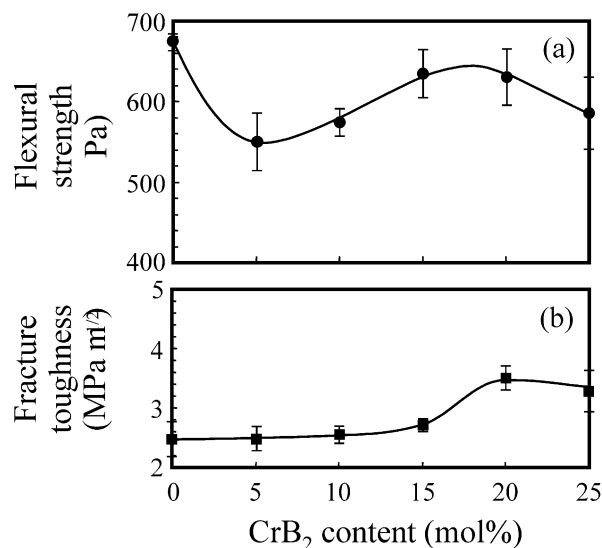


Fig. 5. Mechanical properties of specimens as a function of  $CrB_2$  content: (a) flexural strength and (b) fracture toughness.

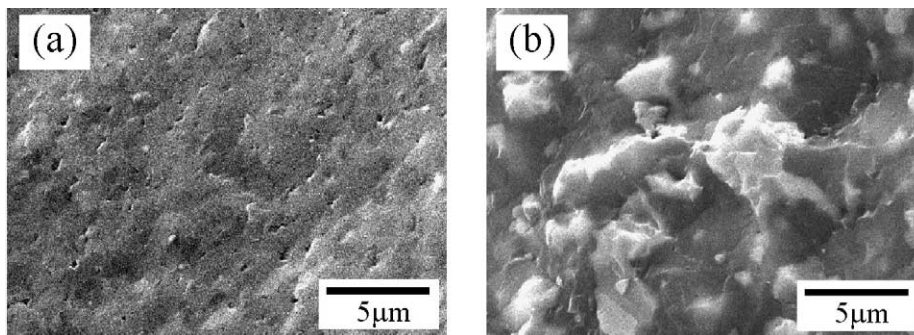


Fig. 6. Fractured surfaces of specimens: (a) specimen without  $\text{CrB}_2$  and (b)  $\text{B}_4\text{C}$ –20 mol%  $\text{CrB}_2$ .

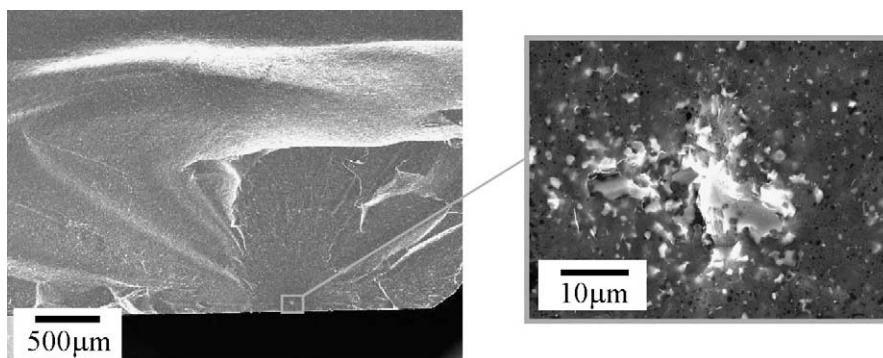


Fig. 7. Fractured surface after bending test for  $\text{B}_4\text{C}$ –5 mol%  $\text{CrB}_2$  specimen.

The thermal expansion coefficient of  $\text{CrB}_2$  is larger than that of  $\text{B}_4\text{C}$ ,<sup>1</sup> such that residual stress is generated around the  $\text{CrB}_2$  particles during cooling. It seems that this residual stress results in the formation of microcracks and, to some degree, deflection of propagating cracks, and leads to improved fracture toughness of the composite materials.<sup>17–20,25</sup>

As shown in Fig. 5a, the specimen without  $\text{CrB}_2$  exhibited the highest strength of 675 MPa. This value is higher than the strength of monolithic  $\text{B}_4\text{C}$  ceramics reported in previous works.<sup>8,9,11</sup> It seems that the high flexural strength obtained in the present work is attributed to the very fine grained microstructure shown in Fig. 1. The variation of strength with  $\text{CrB}_2$  content was complicated. The flexural strength decreased initially to 551 MPa with the addition of 5 mol%  $\text{CrB}_2$ , then increased with  $\text{CrB}_2$  content in the range between 5 and 15 mol%. However,  $\text{CrB}_2$  contents greater than 20 mol% led to reduction in strength. High strength of over 630 MPa was obtained for  $\text{CrB}_2$  contents of 15 and 20 mol%. In particular, both high strength of 630 MPa and modest fracture toughness of 3.5  $\text{MPa m}^{1/2}$  could be achieved in the specimen with 20 mol%  $\text{CrB}_2$ . The fractured surface of the  $\text{B}_4\text{C}$ –5 mol%  $\text{CrB}_2$  specimen after bending test is shown in Fig. 7. It can be seen that the fracture origin was an aggregation of  $\text{CrB}_2$  particles. The decrease in the flexural strength by the addition of 5 mol%  $\text{CrB}_2$  may be caused by the increase in flaw size

due to the aggregated  $\text{CrB}_2$  particles. The flexural strength increases with further addition of  $\text{CrB}_2$  owing to the improvement of the fracture toughness. It was assumed that the reduction of flexural strength with the addition of 25 mol%  $\text{CrB}_2$  was attributed to the shortening of the average of interparticle spacing which leads a large flaw size by the connecting of microcracks.<sup>25</sup>

In this study, the  $\text{CrB}_2$  particle size was relatively larger than the  $\text{B}_4\text{C}$  grain size. It has been reported that the size of the dispersed particles remarkably influences the flexural strength and the fracture toughness for two phase composites.<sup>25</sup> Future studies will therefore concentrate on optimizing the  $\text{CrB}_2$  particle size.

#### 4. Conclusions

$\text{B}_4\text{C}$ – $\text{CrB}_2$  ceramic composites were fabricated by hot-pressing powder mixtures of fine  $\text{B}_4\text{C}$  powder and 0–25 mol%  $\text{CrB}_2$  particulate. The hot-pressed specimens exhibited a composite microstructure where  $\text{CrB}_2$  particles of a few micron were dispersed in a fine grained  $\text{B}_4\text{C}$  matrix. The fracture toughness increased as the  $\text{CrB}_2$  content increased. Both high strength of 630 MPa and modest fracture toughness of 3.5  $\text{MPa m}^{1/2}$  could be achieved in the specimen with 20 mol%  $\text{CrB}_2$  (13 vol.%). Residual stress is generated around the  $\text{CrB}_2$  particles due to the thermal expansion mismatch. It

seems that this residual stress leads to the formation of microcracks and some deflection of propagating cracks, consequently improving the fracture toughness.

### Acknowledgements

This work has been supported by METI, Japan, as part of the Synergy Ceramics Project. Part of the work has been supported by NEDO. The authors are members of the Joint Research Consortium of Synergy Ceramics. The authors are grateful to Dr. Shuji Sakaguchi (AIST) for valuable comments.

### References

- Nishikawa, H., Powder or boron compound at present. *Ceramics*, 1987, **22**, 40–45.
- Takagi, K., Boride materials. *Metals and Technologies*, 1993, **1**, 23–28.
- Nishiyama, K., Sintering and tribology of boride hard materials. *J. Jpn. Soc. Powder and Powder Met.*, 1996, **43**, 464–471.
- Johnson, W. C., Advanced materials and powders. *Am. Ceram. Soc. Bull.*, 2001, **80**, 64–66.
- Thevenot, F., Boron carbide—a comprehensive review. *J. Eur. Ceram. Soc.*, 1990, **6**, 205–225.
- Thevenot, F., a review on boron carbide. *Key Eng. Mater.*, 1991, **56–57**, 59–88.
- Suzuki, H., Hase, T. and Maruyama, T., Effect of carbon on sintering of boron carbide. *Yogyo-Kyokai-Shi*, 1979, **87**, 430–433.
- Schwetz, K. A. and Grellner, W., The influence of carbon on the microstructure and mechanical properties of sintered boron carbide. *J. Less-Common Met.*, 1981, **82**, 37–47.
- Schwetz, K. A., Sigl, L. S. and Pfau, L., Mechanical properties of injection molded B<sub>4</sub>C–C ceramics. *J. Solid State Chem.*, 1997, **133**, 68–76.
- Kanno, Y., Kawase, K. and Nakano, K., Additive effect on sintering of boron carbide. *Yogyo-Kyokai-Shi*, 1987, **95**, 1137–1140.
- Thevenot, F., Sintering of boron carbide and boron carbide—silicon carbide two—phase materials and their properties. *J. Nucl. Mater.*, 1988, **152**, 154–162.
- Kim, H. W., Koh, Y. H. and Kim, H. E., Densification and mechanical properties of B<sub>4</sub>C with Al<sub>2</sub>O<sub>3</sub> as a sintering aid. *J. Am. Ceram. Soc.*, 2000, **83**, 2863–2865.
- Sigl, L. S., Processing and mechanical properties of boron carbide sintered with TiC. *J. Eur. Ceram. Soc.*, 1998, **18**, 1521–1529.
- Zakhariew, Z. and Radev, D., Properties of polycrystalline boron carbide sintered in the presence of W<sub>2</sub>B<sub>5</sub> without pressing. *J. Mater. Sci. Lett.*, 1988, **7**, 695–696.
- Ruh, R., Kearns, M., Zangvil, A. and Xu, Y., Phase and property studies of boron carbide—boron nitride composites. *J. Am. Ceram. Soc.*, 1992, **75**, 864–872.
- Kim, D. K. and Kim, C. H., Pressureless sintering and microstructural development of B<sub>4</sub>C–TiB<sub>2</sub> based composites. *Adv. Ceram. Mater.*, 1988, **3**, 52–55.
- Sigl, L. S. and Kleebe, H. J., Microcracking in B<sub>4</sub>C–TiB<sub>2</sub> composites. *J. Am. Ceram. Soc.*, 1995, **78**, 2374–2380.
- Tuffe, S., Dubois, J., Fantozzi, G. and Barbier, G., Densification, microstructure and mechanical properties of TiB<sub>2</sub> ampinus; B<sub>4</sub>C based composites. *Int. J. Refr. Metals Hard Mater.*, 1996, **14**, 305–310.
- Skorokhod, V., Vljajic, M. D. and Krstic, V. D., Mechanical properties of pressureless sintered boron carbide containing TiB<sub>2</sub> phase. *J. Mater. Sci. Lett.*, 1996, **15**, 1337–1339.
- Skorokhod, V. and Krstic, V. D., High strength-high toughness B<sub>4</sub>C–TiB<sub>2</sub> composites. *J. Mater. Sci. Lett.*, 2000, **19**, 237–239.
- Iizumi, K., Yoshikawa, N., Kudaka, K. and Okada, S., Sintering of chromium borides synthesized by solid-state reaction between metallic chromium and amorphous boron. *J. Jpn. Soc. Powder Powder Met.*, 1999, **46**, 710–714.
- Iizumi, K., Shikada, G., Kudaka, K. and Okada, S., Sintering of Cr<sub>1-x</sub>Mo<sub>x</sub>B<sub>2</sub> ceramics. *J. Jpn. Soc. Powder Powder Met.*, 1997, **44**, 222–226.
- Ordanyan, S. S. and Dmitriev, A. I., Reaction in the B<sub>4</sub>C–B<sub>2</sub>Cr system. In *Handbook of Ternary Alloy Phase Diagrams*, Vol. 10, ed. Villars, P., Prince, A. and Okamoto, H. ASM international, OH, USA, 1995, pp. 5327.
- Nose, T. and Fujii, T., Evaluation of fracture toughness for ceramic materials by a single-edge-precracked-beam method. *J. Am. Ceram. Soc.*, 1988, **71**, 328–333.
- Yasuoka, M., Brito, M. E., Hirao, K. and Kanzaki, S., Effect of dispersed particle size on mechanical properties of alumina/non-oxides composites. *J. Ceram. Soc. Jpn.*, 1993, **101**, 889–894.